ACS OMEGA

http://pubs.acs.org/journal/acsodf

Article

Designing Excess Electron Compounds by Substituting Alkali Metals to a Small and Versatile Tetracyclic Framework: A Theoretical Perspective

Santosh Kumar Yadav, Snehasis Bhunia, Rajneesh Kumar, Ritu Seth, and Ajeet Singh*

Cite This: *ACS Omega* 2023, 8, 7978−7988

Read Online

ACCESS | Metrics & More | Article Recommendations | Supporting Information

ABSTRACT: Organic compound-based nonlinear optical (NLO) materials have sparked a lot of attention due to their multitude of applications and shorter optical response times than those of inorganic NLO materials. In the present investigation, we designed exo-exo-tetracyclo[6.2.1.1^{3,6}.0^{2,7}]dodecane (TCD) derivatives, which were obtained by replacing H atoms of methylene bridge carbon with alkali metals (Li, Na, and K). It was observed that upon the substitution of alkali metals at bridging CH_2 carbon, absorption within the visible region occurred. Moving from **1** to **7** derivatives, the maximum absorption wavelength of the complexes exhibited a red shift. The designed molecules showed a high degree of intramolecular charge transfer (ICT) and excess electrons in nature, which were responsible for rapid optical response time and significant large molecular (hyper)polarizability. Calculated trends also inferred that the crucial transition energy decreased in order that also played a key role in the higher nonlinear optical response. Furthermore, to examine the effect of the structure/property relationship on the nonlinear optical properties of these investigated compounds (**1**−**7**), we calculated the density of state (DOS), transition density matrix (TDM), and frontier molecular orbitals (FMOs). The largest first static hyperpolarizability (β_{tot}) of TCD derivative **7** was 72059 au, which was 43 times greater than that of the prototype p-nitroaniline (β_{tot} = 1675 au).

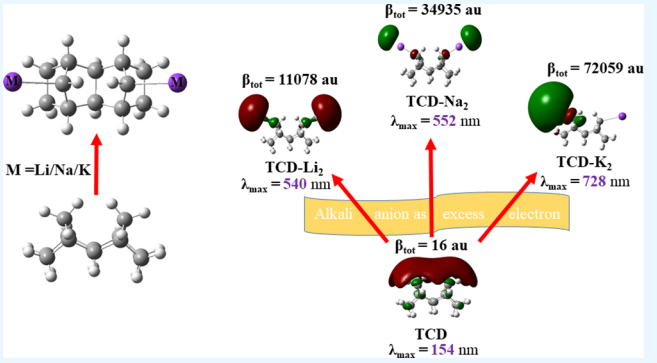

1. INTRODUCTION

The scientific community has shown strong interest in designing and synthesizing nonlinear optical (NLO) materials over the last three decades due to their promising applications in optical logic, optical communication, and optical computing. It is also employed in advanced photonics, dynamic image processing, and laser-based technologies.[1−10] A significant amount of effort has been done into the discovery of high-performance NLO organic compounds.[11−16] There are numerous methods and approaches for achieving the goal; however, quantum chemical calculations play a significant role in the search for new and novel NLO materials with high hyperpolarizabilities.[17−23] With the introduction of new computer structural design and more practical incorporation of quantum chemical approaches such as Møller−Plesset perturbation (MP2) theory, it has become viable to apply these methods in the design of nonlinear optical molecules or to understand the factors and structure−property relationships that are liable for increasing hyperpolarizability values.[24]

Organic-based nonlinear optical compounds have a broad range of applications from catalysis to optoelectronics.[25] It is noticed that the NLO properties can be modulated in several ways such as by metal−ligand frameworks,[26] push−pull mechanism,[27,28] and introduction of excess electrons.[29] Among the recommended approaches for improving the NLO response, the designing and simulation of excess electron organic compounds are the dynamic areas of research.[30,31] Alkali metals,[32,33] alkali earth metals,[34,35] superalkali,[32,36] and transition metals[37,38] can be used to create diffuse surplus electrons in complexes. It is worth noting that more electrons boost the nonlinear optical response by lowering transition energy and allowing for considerable charge transfer in organic molecules.[39] The excess electron compounds are found in diffuse molecular orbitals, which are outside of the parent molecules.[40] Several literature reports showed that the doping of inorganic nanocages with alkali metal atoms resulted in an extraordinarily high NLO response.[41] Such findings revealed that capping of inorganic systems with alkali metal atoms considerably increased their hyperpolarizability. Organic systems can improve the NLO behavior by capping, similar to inorganic systems by suitable substitution with alkali metals.

Received: December 7, 2022
Accepted: January 26, 2023
Published: February 16, 2023

Table 1. Important Bond Lengths (Å) of Fully Optimized 1−7 Molecules Calculated at the MP2-6-311+G(d,p) Level of Theory[a]

bond length	1	2	3	4	5	6	7
C···C (bridging)	3.126	3.179	3.225	3.154	3.149	3.171	3.177
H···H (bridging)	1.779	1.739	1.697	1.748	1.721	1.752	1.730
C−H	1.097[cB]						
C−Li		2.036	2.039[cB]				
C−Na				2.401	2.411[cB]		
C−K						2.725	2.736[cB]
E_{gap} (eV)	12.51	7.05	6.28	6.13	5.30	5.61	4.57
λ_{max}	154.04	472.50	540.78	464.94	552.54	576.99	728.06
$q(X^C)$	0.173	0.884	0.867[b]	0.809	0.758[b]	0.907	0.865[b]

[a]TD-DFT method was used to obtain the maximum absorption wavelengths (nm) for **1**−**7**. [b]$q(X^C)$: the NBO charge. [cB]ond length values are the same for (two alkali metals substituted) alkali metal and carbon to alkali metal bonds.

A recent literature report revealed that by replacing the H atom at the methine position in adamantane with an alkali metal (Li, Na, or K), a substantial enhancement in the nonlinear response was observed. The hyperpolarizability values of the resultant alkali metal complexes were many times higher than that of the isolated adamantine molecule.[42] Based on this observation and fact, it can be concluded that alkali metal doping significantly improves the optoelectronic characteristics of both inorganic and organic systems.

TCD is rigid and has only sigma bond cycloalkanes, which can be considered a nanometer-sized H-terminated 2D material.[43,44] More than five decades ago, Winstein et al. prepared several polycyclic hydrocarbons.[45] Ermerhas reported crystal structure analysis on the derivatives of exo-exo-tetracyclo[6.2.1.1^{3,6}.0^{2,7}]dodecanols.[46] Fused[n]-polynorbornane-based frameworks appear to be one of the most useful and well-organized macromolecular scaffolds that may be customized for specific applications.[47]

In the quest for the large first hyperpolarizability of the organic scaffold, we used the TCD compound as a parent molecule, and other molecules were designed by suitable substitution of an alkali metal at an appropriate position to the parent scaffold.[48] We employed quantum chemical calculations to evaluate the unusual first hyperpolarizability of these designed molecules. Quantum chemical calculations show that the proper replacement of TCD by alkali metals causes absorption in the visible region. From Li to K derivatives, the maximum absorption wavelength of the complexes shows a red-shift trend. The calculated results indicate that the transition energy decreases as a result of the TCD derivatives showing a substantial increase in nonlinear optical sensitivity. Further, we also performed frontier molecular orbitals, density of states (DOS), transition density matrix (TDM), and molecular electrostatic potential (MESP) calculations (see the Supporting Information and Figure S1), which further substantiate our findings.

2. COMPUTATIONAL DETAILS

The optimized geometrical structure of the designed molecules (**1**−**7**) with real frequencies in the ground state was obtained by the MP2/6-311+G(d,p) method. The static (hyper)-polarizabilities were evaluated at the same level of theory. The static first hyperpolarizabilities were evaluated by a finite-field (FF) approach of the MP2 method.[24] A recent literature report regarding NLO calculations revealed that the Møller−Plesset perturbation (MP2) calculated results were in close proximity to the calculated results from more sophisticated correlation methods.[24] For comparison of MP2 calculated results, we also performed DFT calculations by applying different functions, Supporting Information. We used a 0.001 au applied electric field for the evaluation of static first-order hyperpolarizability, which is well established to the adequate value for numerical differentiation. The absorption spectra were calculated at the TD-DFT/6-311+G (d,p) level of theory.

The average polarizability (α_0) can be calculated as follows

$$\alpha_0 = \frac{1}{3}(\alpha_{xx} + \alpha_{yy} + \alpha_{zz}) \quad (1)$$

The first hyperpolarizability is obtained as follows

$$\beta_{tot} = (\beta_x^2 + \beta_y^2 + \beta_z^2)^{1/2} \quad (2)$$

where

$$\beta_i = (\beta_{iii} + \beta_{ijj} + \beta_{ikk})i, j, k = x, y, z \quad (3)$$

In Table 2, the calculated parameters illustrated above, the electronic dipole moment $\{\mu_i\ (i = x, y, z)\}$, and the total dipole moment (μ_{tot}) for the title compounds are listed. The total dipole moment is calculated by the following equation:

$$\mu_{tot} = (\mu_x^2 + \mu_y^2 + \mu_z^2)^{1/2} \quad (4)$$

The net dipole moment, mean polarizability (α_0), and first static hyperpolarizability (β_{tot}) were performed by the Gaussian 16 program package.[49]

3. RESULTS AND DISCUSSION

3.1. Geometrical Parameters. All of the designed molecules (**1**−**7**) were optimized by the MP2/6-311+G(d,p) level of theory. All of the ground-state geometries were verified as global minima by vibrational frequency analysis at the same level of theory, since negative vibrational frequencies were absent in all of the cases.

The important geometrical parameters are listed in Table 1. To validate our method and basis set, we compared our calculated geometry with the experimental finding to gauge whether our geometry was reasonable. The C−X (X = H, Li, Na, and K) bond lengths of TCD derivatives (**2**−**7**) show interesting variations compared with those of TCD. The C−X bond length is in increasing order as the metal atomic number increases (Table 1). Experimentally, the observed C···C and H···H distances for bridging CH_2 groups are 3.104 and 1.82 Å, respectively. These values are in good accordance with the corresponding values calculated in this work, which are 3.126 and 1.78 Å, respectively. Thus, the MP2 method with the 6-

https://doi.org/10.1021/acsomega.2c07743
ACS Omega 2023, 8, 7978−7988

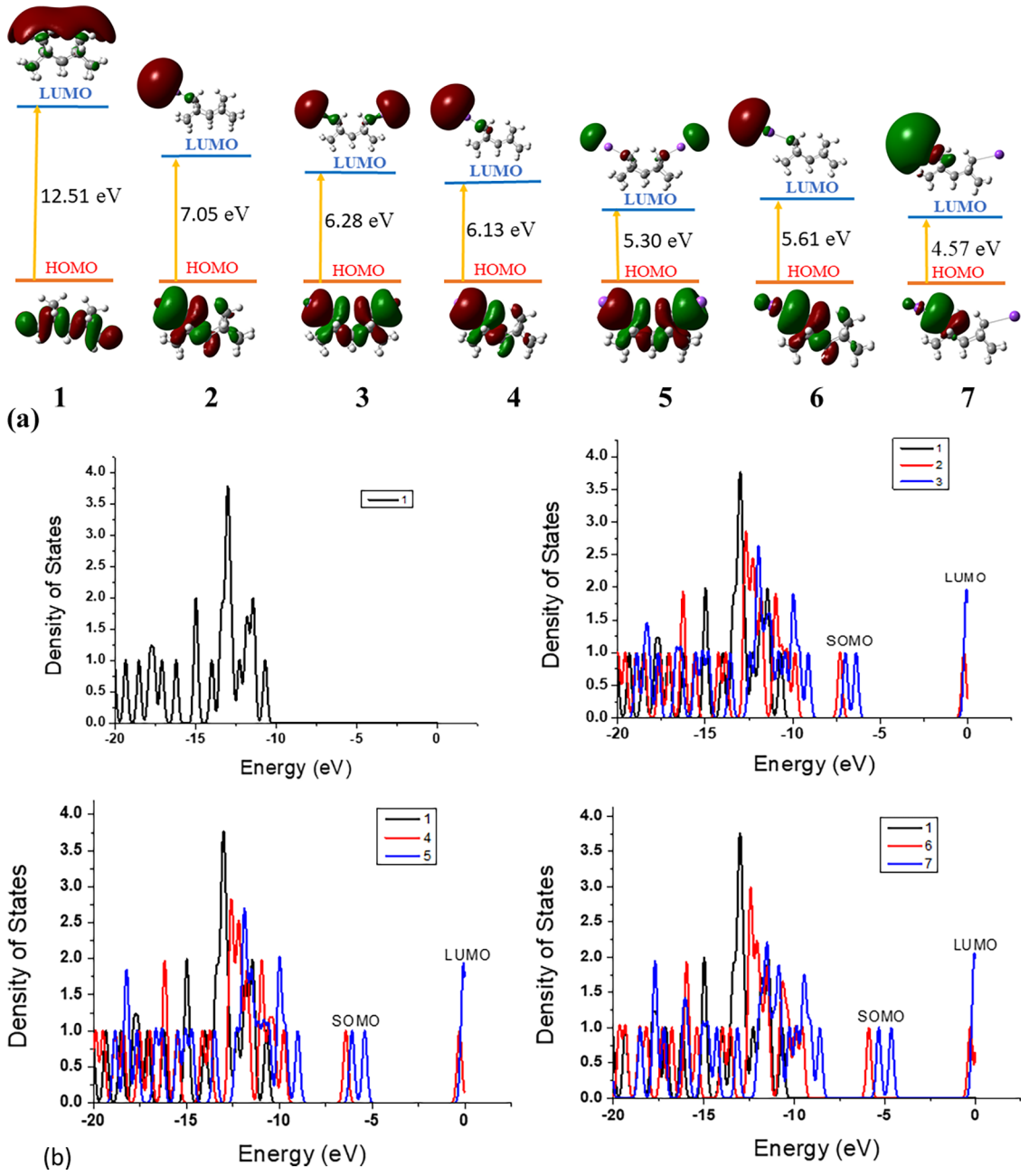

Figure 1. (a) Frontier molecular orbitals of **1**−**7** at the MP2/6-311+G(d,p) level of theory with an isosurface value of 0.02 au. (b) DOS curves for **1**−**7**.

311+G(d,p) basis set seems to be adequate for further calculations. Other significant geometrical parameters also infer that the geometry of TCD is reasonable as on substitution of alkali metal shows a very minor deviation, which is given in Table 1. The computed results indicate that the outer bridging CH_2 hydrogen substitution by an alkali metal is more energetically favored than that of the inner one (see Table S1 in the Supporting Information). Table 1 also infers that the bond length of C−K (2.736) is more than those of C−Na and C−Li.

3.2. Charge Transfer and Electronic Properties. To see the intramolecular charge transfer, we performed a natural population scheme[50] for atomic charges on alkali metals present in TCD derivates. Based on atomic charge analysis, the metals Li, Na, and K carry higher charges than TCD bridging CH_2 hydrogen (Table 1). It is interesting to note that the monosubstituted alkali metal TCD derivatives bear higher atomic charges than disubstituted alkali metal TCD derivatives; however, disubstituted alkali metal TCD derivatives have equal atomic charges on both alkali metals (Table 1). The natural charges of alkali metals (Li, Na, K) in TCD derivatives are in the range of 0.758−0.907|e|, which infers strong charge transfer. Such a feature has already been found in the instance of adamantane substituted with an alkali metal and Ti@C_{28}.[51] It is noted that the intramolecular charge transfer is directly connected to the NLO response of systems.[52,53]

To obtain more insights into the charge transfer and electronic properties, we analyzed FMOs. The transitions in FMOs that are highest occupied molecular orbitals (HOMOs) and lowest unoccupied molecular orbitals (LUMOs) are one

https://doi.org/10.1021/acsomega.2c07743
ACS Omega 2023, 8, 7978−7988

Table 2. Values of α_0 (au) and β_{tot} (au) of TCD Derivatives were Calculated at the MP2/6-311+G (d,p) Level of Theory[a]

	1	2	3	4	5	6	7
α_0	123	148	189	187	311	189	377
β_x	−5	−4996	0	−19 890	3	28 058	11
β_y	15	−1	11 078	−7918	34 935	−6592	72 059
β_z	0.00	3315	4	0	0	−1	0
β_{tot}	16	5972	11 078	21 408	34 935	28 822	72 059
f_o	0.0263	0.1010	0.1585	0.3237	0.4474	0.1928	0.3586
ΔE	8.0487	2.6240	2.2927	2.6667	2.2439	2.1488	1.7029
μ_g	0.0932	6.3869	6.3865	6.5988	6.1141	8.5976	5.7092
μ_e	2.1052	5.4981	0.4020	1.7476	1.8172	0.8861	2.5710
$\Delta\mu$	2.012	0.8888	5.9845	4.8512	4.2969	7.7115	3.1382
transition nature	H-2 → L	H → L	H → L	H→ L	H → L	H → L	H → L

[a]The differences in the dipole moments between the ground and excited states ($\Delta\mu$), the transition energies (ΔE), and the oscillator strength (f_0) are determined by the TD-DFT method.

Scheme 1. (a) Optimized Structure of TCD and Important Bond Length Given in Å; (b) Structures of a TCD Molecule and Its Derivatives (1−7)

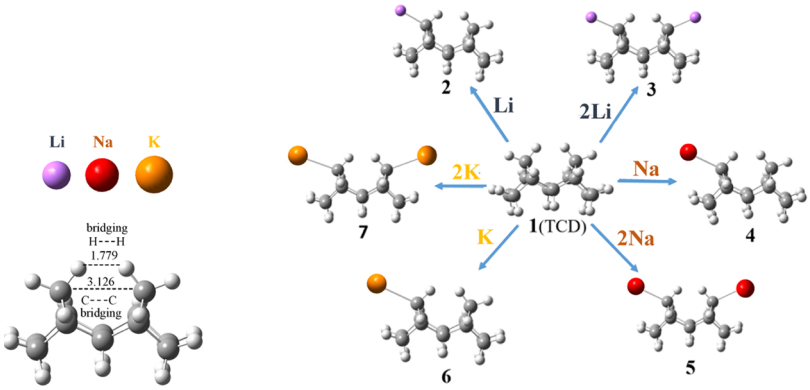

(a) (b)

of the key factors in determining the optoelectronic properties of any molecule. The calculated energy gaps of molecules **1**−**7** are presented in Table 1. Upon substitution of TCD with alkali metals, the crucial transitions of **2** to **7** are from the HOMO to LUMO energy level. The electron clouds of LUMOs in **2**−**7** have the same pattern and are mainly located on the alkali metal side (Figure 1). However, an unusual observation was seen in the case of **7**. In this designed molecule, the electron cloud was observed only on one side of bridging carbon in LUMO, which was not in the cases of **3** and **5**. This observation indicates that the other transitions are possible, which are discussed in the following section. When we see the HOMOs critically, it is revealed that alkali metal atoms (Li, Na, and K) have large diffuse orbitals, and their valence electrons are loosely bound to the complexes. In general, the valence electrons of Li, Na, and K become more and more diffused in the order of Li < Na < K, which makes the transitions easier. As a consequence, ΔE values of **2**, **3**, **4**, **5**, **6**, and **7** are much smaller than that of TCD (**1**), leading to larger β_{tot} values.

Further, to validate the electronic properties of the designed complexes, we performed density of state (DOS) analysis using GaussSum software.[54] The DOS spectra of our designed TCD derivatives were revealed as excess electron compounds and are given in Figure 1b. To see the intricate features of charge transfer and electronic properties, we calculated the highest occupied molecular orbitals (HOMOs), which are the singly occupied molecular orbitals (SOMOs) in the case of alkali metal-substituted TCD. In the ground state, the HOMO energy of compound **1** is −10.67 eV, which upon excitation increases to 1.84 eV, and the band gap between the HOMO and LUMO is found to be 12.51 eV. It is noted that the calculated DOS spectra have no evidence for SOMO in parent molecule **1**. However, in the latter case (**2**−**7**), the SOMO was observed. Similarly, the SOMO and LUMO of compound **2** have energies of −7.29 and −0.24 eV, respectively, with a band gap of 7.05 eV. Other compounds **3**, **4**, **5**, **6**, and **7** have energies of −6.36, −6.40, −5.38, −5.87, and −4.63 eV, respectively, in the ground state, while their excited-state energies (LUMO) are found to be −0.08, −0.27, −0.08, −0.26, and −0.06 eV, with band gaps (ΔE_g) of 6.28, 6.13, 5.30, 5.61, and 4.57 eV, respectively. We plotted the DOS spectra of all derivatives, which are shown in Figure 1b. The calculated DOS curves infer that the alkali atom contributes to the SOMOs. Therefore, the reduced E_{gap} of TCD derivatives may result due to a rise in the SOMO level. This smaller E_{gap} may suggest that the electrical conductivity of TCD derivatives is significantly improved.

3.3. Nonlinear Optical Properties and Electronic Transitions Analysis. The mean polarizability (α_0) and ground-state and excited-state dipole moments (μ_g and μ_e, respectively) of the designed molecules (**1**−**7**) were computed at the MP2/6-311+G(d,p) level of theory, and the calculated values are given in Table 2. The dipole moment in the ground

https://doi.org/10.1021/acsomega.2c07743
ACS Omega 2023, 8, 7978−7988

Table 3. Hyperpolarizability (β_{tot} in au) of the Designed Molecules is Evaluated Analytically Using Hybrid and Dispersion-Corrected DFT with Different Functionals and the MP2 Method using the 6-311+G(d,p) Basis Set

compounds	M062X	CAM-B3LYP	WB97XD	BHandHLYP	APFD	B97D	MP2
1	15.80	15.89	18.91	11.49	17.35	22.70	16.71
2	5327.52	4472.29	4680.69	4093.40	5834.75	13 548.05	5996.98
3	11 701.86	7339.18	8245.07	7086.51	10 609.30	27 201.07	11 078.20
4	21 147.10	10 639.32	10 639.35	11 528.16	15 168.13	21 895.59	21 408.32
5	46 674.62	11 577.48	22 397.78	16 524.52	22 656.01	30 238.95	34 935.46
6	11 646.83	18 239.21	15 669.29	19 571.83	27 160.62	48 674.22	28 822.18
7	28 397.07	26 829.31	30 428.89	30 806.44	44 715.54	69 952.88	72 059.95

state (μ_g) of **1** is negligibly small (μ_g = 0.0932 D), as expected due to the symmetric charge distribution. However, μ_g values of TCD derivatives significantly increase (Table 2). These values are consistent with the charge distribution and geometry of these molecules (Scheme 1). In a similar line, α_0 significantly increases from **1** to **7**. These calculated values were correlated well with charge transfer in these systems (see Table 1). In view of the hardness principle, species with lower energy gaps are less hard and thus more polarizable. As a result, these α_0 values are in good agreement with the E_{gap} values of substituted TCD derivatives.

The NLO behavior of alkali-substituted TCD complex (Li, Na, and K) systems has been explored by computing their first hyperpolarizabilities (β_{tot}) at the MP2/6-311+G(d,p) level, which are listed in Table 2. Upon substitution of bridging CH_2 carbon of TCD by alkali metals remarkably enhances the β_{tot} value. The calculated results indicate that the substitution of alkali metals obviously affects the first hyperpolarizability of TCD derivatives. Notably, the largest β_{tot} value of **7** (72 059) is about 43 times larger than that of the prototypical second-order NLO of p-nitroaniline (β_{tot} = 1675 au). The calculated enhanced β_{tot} values of TCD derivatives advocate their strong NLO behavior.

To check the consistency in the calculations of polarizability and hyperpolarizabilities values, the appropriate choice of proper methods and basis sets is important to obtain unswerving results. Therefore, we calculated the average polarizability and first hyperpolarizability of the designed molecules using a variety of hybrid and dispersion-corrected DFT functionals such as M062X/6-311+G(d,p), CAM-B3LYP,[55] BHandHLYP,[56] WB97XD,[57] APFD,[58,59] and B97D[60] using the 6-311+G(d,p) basis set as well as the MP2 method using the 6-311+G(d,p) basis set. The calculated β_0 values at M062X,[61] CAM-B3LYP, WB97XD, BHandHLYP, APFD, and B97D using the 6-311+G(d,p) basis set along with MP2 at the same basis set are not consistent.[62−65]

The reference molecule (p-nitroaniline) was also calculated at the same level of theory and functional. Calculated results suggest that DFT-based functionals M062X and CAM-B3LYP and the MP2 method have a very close agreement for average polarizability and first hyperpolarizability values, and it is also seen with simply designed molecule **1**. However, when we are turning from a simpler push−pull organic system into excess electrons, then we observed a larger deviation with DFT hybrid functionals. It is important to note that as we have taken the dispersion-corrected functional, the calculated first hyperpolarizability becomes closer to MP2 method calculations (see Table 3 and Figure 2). The calculated β_0 values of **1**−**7** by MP2 are significantly larger than M062X, CAM-B3LYP, and WB97XD results but closer to the B97D value. The B97D-calculated β_0 of the molecule fairly agrees with the MP2 method-calculated β_0. Among the chosen methods (Table 3), the calculated β_0 value with the M062x functional is not consistent, as it is apparent that excess electron dispersion correction is poorly estimated by this functional. However, the long-range corrected functional properly estimates the dispersion interactions, which are very close to those calculated by the MP2 method. Dispersion interactions are a ubiquitious consequence of electron correlation. Excess electron compounds are found in diffuse molecular orbitals, which are outside of the parent molecules. Therefore, the calculated results are underestimated when we use the hybrid DFT functional; however, when we use the dispersion-corrected DFT functional, the calculated results are close to the MP2 method calculations.

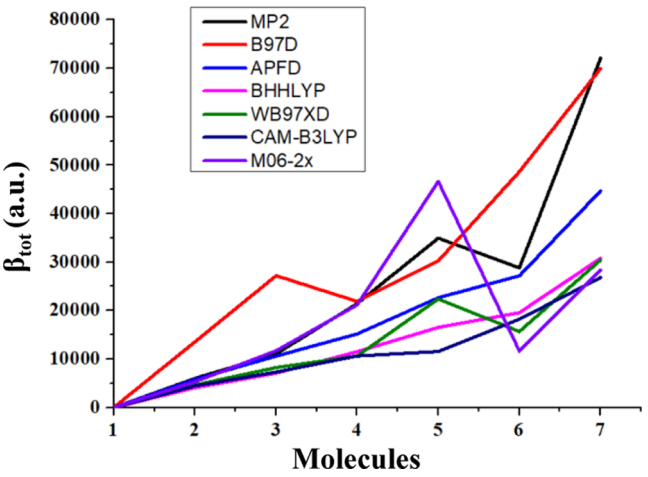

Figure 2. Plot of the first static hyperpolarizability (β_{tot}) values of the designed TCD molecules.

A previous literature report also revealed such variations. Champagne et al.[66] showed that the hybrid functional BHandHLYP minimizes the overestimation of the NLO property. Nakano et al.[67] noted that the CCSD(T) results of hyperpolarizability can be reproduced by the BHandHLYP method. Thus, the latter method can be chosen especially for larger systems, as the CCSD(T) method is computationally very costly and quite difficult to perform. The BHandHLYP, WB97XD, APFD, and B97D functionals are also used widely for evaluating the first hyperpolarizability for alkali and alkaline earth metal-doped systems. Thus, for the investigated molecular system, the chosen DFT functionals APFD and B97D can provide satisfactory results, which are close to the MP2 method-calculated results (Table 3). Thus, we employed the MP2 method for the present investigation.

In the case of monosubstituted alkali halide TCD derivatives, the β_{tot} values are relatively lower than those of disubstituted alkali halide TCD derivatives (see Table 2). It is

https://doi.org/10.1021/acsomega.2c07743
ACS Omega 2023, 8, 7978−7988

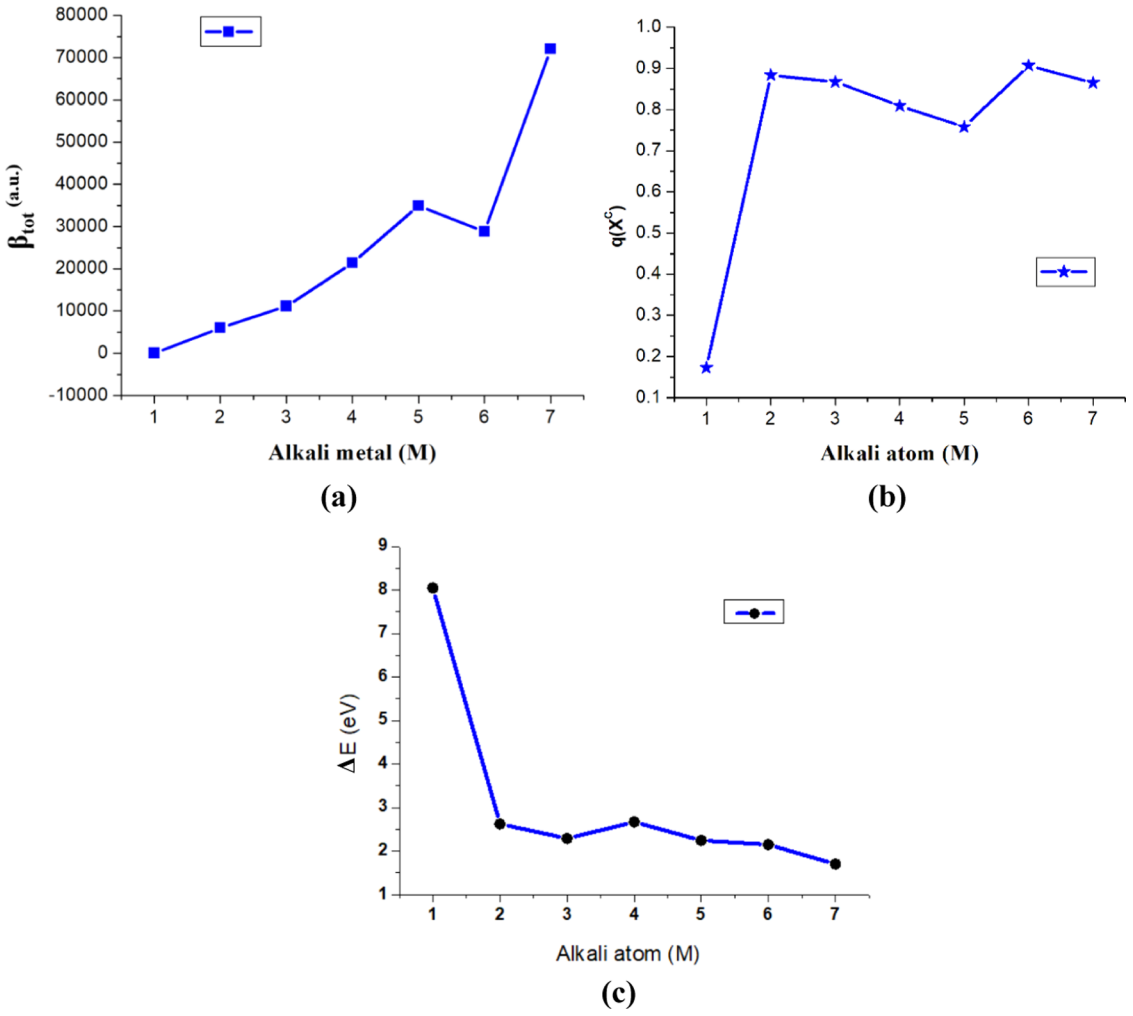

Figure 3. Plots of the first static hyperpolarizability (β_{tot}) (a), charge on the alkali metal ($q(X^C)$) (b), and transition energy (ΔE) values (c) of TCD molecules.

observed that the β_{tot} values follow a nearly similar trend as that of charges on the alkali metal (see Table 1) except for compound **7**; however, disubstituted (**7**) metals have equal charges. To analyze this, we plot the β_{tot} values of TCD derivatives and their $q(X^C)$ and ΔE values in Figure 3. It can be seen from Table 1 that the NBO charges of molecules **2**−**7** vary in the range of 0.758−0.907, which are larger than that of molecule **1** (0.173). Molecular electrostatic potential (MESP) calculated results (**1**−**7**) also infer that the charge is mainly localized at the metal-substituted side (see Figure S1 in the Supporting Information). This is consistent with the concept that the NLO response of a system can be improved more efficiently by incorporating excess electrons, as observed previously in a number of investigations.[29] The f_0, $\Delta\mu$, and ΔE values determined at the TD-DFT/6-311+G(d,p) level of theory are listed in Table 2. The crucial electronic transition was specified by the largest oscillator strength (f_0). To predict the origin of β_{tot}, Oudar and Chemla established a simple link between β_{tot} and a low-lying charge transfer transition by the following two-level expression[68,69]

$$\beta_{tot} \propto \frac{\Delta\mu f_0}{\Delta E^3} \quad (5)$$

According to the two-level proposal, the β_{tot} value is proportional to the difference between the dipole moments of the ground state, transition dipole moment ($\Delta\mu$), and the oscillator strength (f_0) but inversely proportional to the third power of the transition energy (ΔE). From the two-level expression (eq 5), it is evident that the transition energy is one of the prominent factors for enhancing the first hyperpolarizability.

Figure 4 depicts the plotted absorption spectra of **1**−**7** complexes. It is worth mentioning that the parent molecule TCD (**1**) exhibits no absorption in the wavelength range of 200−800 nm. However, when bridging CH_2 groups in the TCD is substituted by alkali metals that affect the absorption spectra (Figure 4). The calculated results prompted us to investigate and design TCD derivatives (**2**−**7**). The calculated absorption spectra reveal that the maximum absorption wavelengths of **2**−**7** are significantly higher than that of TCD (λ_{max} = 154.04 nm; see Table 1). According to these findings, λ_{max} shows an apparent bathochromic change with increasing atomic numbers (substituted alkali metal). Surprisingly, the bathochromic shift in λ_{max} can result in reduced transition energies, which may result in larger nonlinear optical responses.

The crucial excited states of all designed TCD derivatives correspond to the transition from HOMO to LUMO, and other possible transitions are shown in Figure 5. Along the prominent transition from HOMO to LUMO, the HOMO and

https://doi.org/10.1021/acsomega.2c07743
ACS Omega 2023, 8, 7978−7988

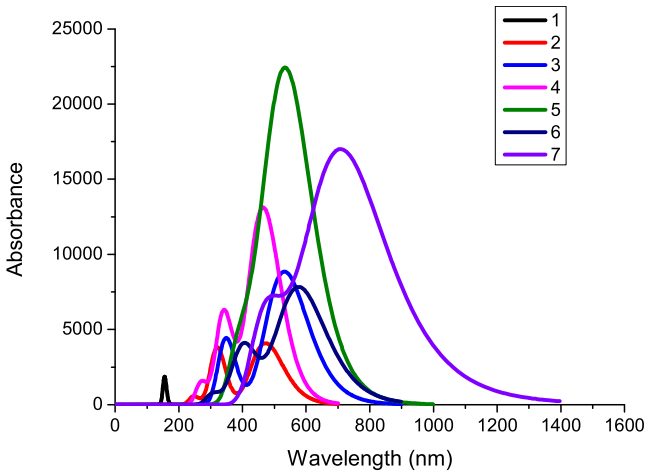

Figure 4. Computed maximal absorption spectra for compounds **1**−**7**.

HOMO-2 to LUMO, LUMO + 1, and LUMO + 3 transitions are also possible (Figure 5). The percent transition probabilities are given in Table S3 (See the Supporting Information).[70] The ΔE values determined at the TD-DFT/6-311+G(d,p) level of theory are listed in Table 2. The ΔE value of **1** is 8.0487, while the ΔE values of **2**, **3**, **4**, **5**, **6**, and **7** are 2.6240, 2.2927, 2.6667, 2.2439, 2.1488, and 1.7029 eV, respectively. The calculated results revealed that the substitution of alkali metals on TCD derivatives greatly reduced the ΔE value. The calculated β_{tot} values followed a similar trend as ΔE values. Thus, ΔE values are in line with the explanation of the variation in β_{tot} values. Similarly, the calculated $\Delta\mu$ values infer that the charge transfer increases from **1** to **7**, which is in accordance with the β_{tot} values. Therefore, $\Delta\mu$ is also an important factor causing the variation in β_{tot} for the designed molecules.

3.4. Transition Density Matrix. We also used Multiwfn 3.8 software[71] to create color 3D transition density matrix (TDM) plots of our designed molecules at the MP2/6-311+G(d,p) level of theory to estimate and visually see charge transfer behavior between the lower and middle energy peaks. It also contains information on the precise placement of electrons, holes, and electron−hole overlap.[72] The TDM plots reveal a great deal about the phenomenon of intramolecular charge transfer (ICT). It is worth noting that our computed molecules have a permissible level of ICT behavior. The heat map reveals that there is robust electron and hole dispersion.

To see the electron−hole distribution, we examined the *X*-axis (corresponding to the hole position) and the *Y*-axis (corresponding to the electron position). In the molecule of TCD (**1**), electrons and holes are equally distributed on the whole isosurface, and in **2**, **4**, and **6** molecules, electrons and holes are present on the diagonal of the surface at an index of

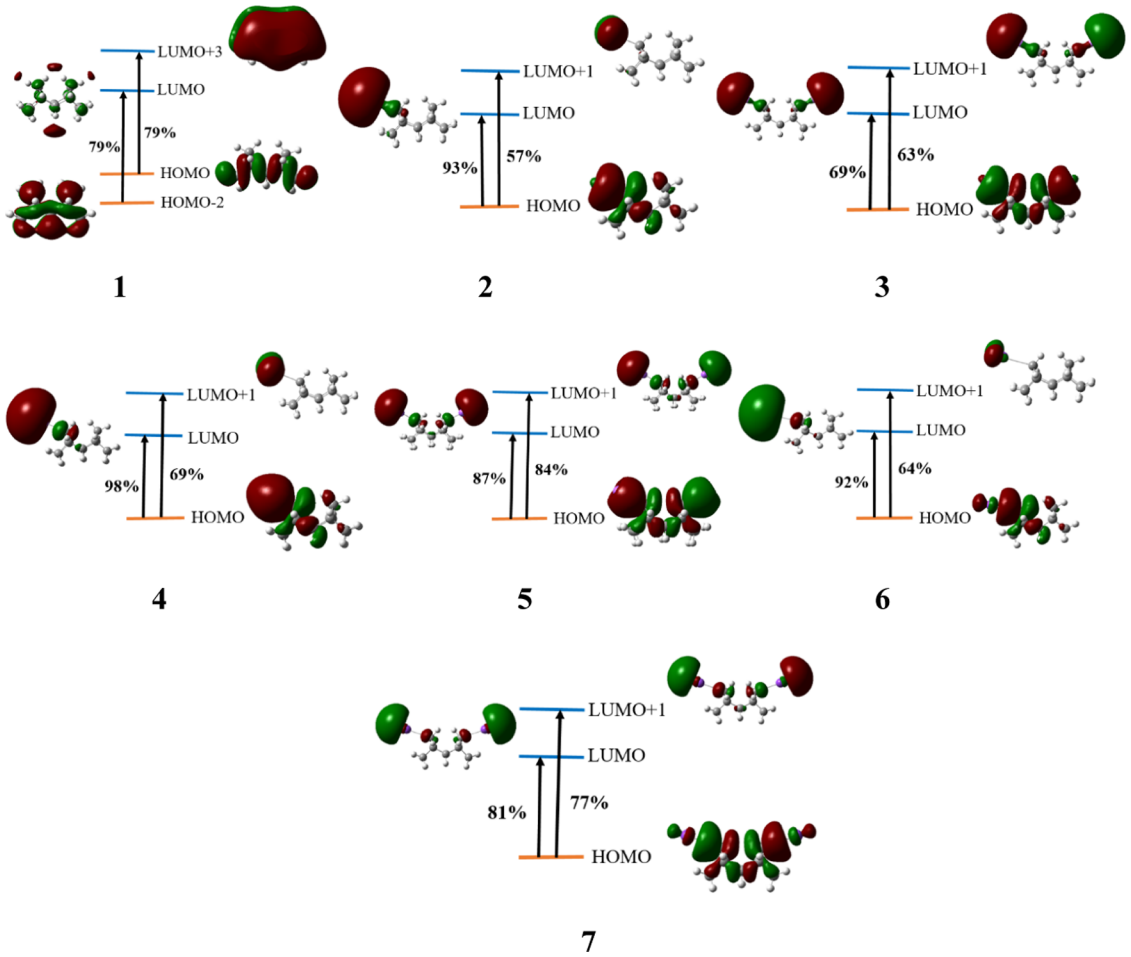

Figure 5. Crucial electronic transition and molecular orbital involved along with transition probabilities are calculated using the TD-DFT/6-311+G(d,p) level of theory.

https://doi.org/10.1021/acsomega.2c07743
ACS Omega 2023, 8, 7978−7988

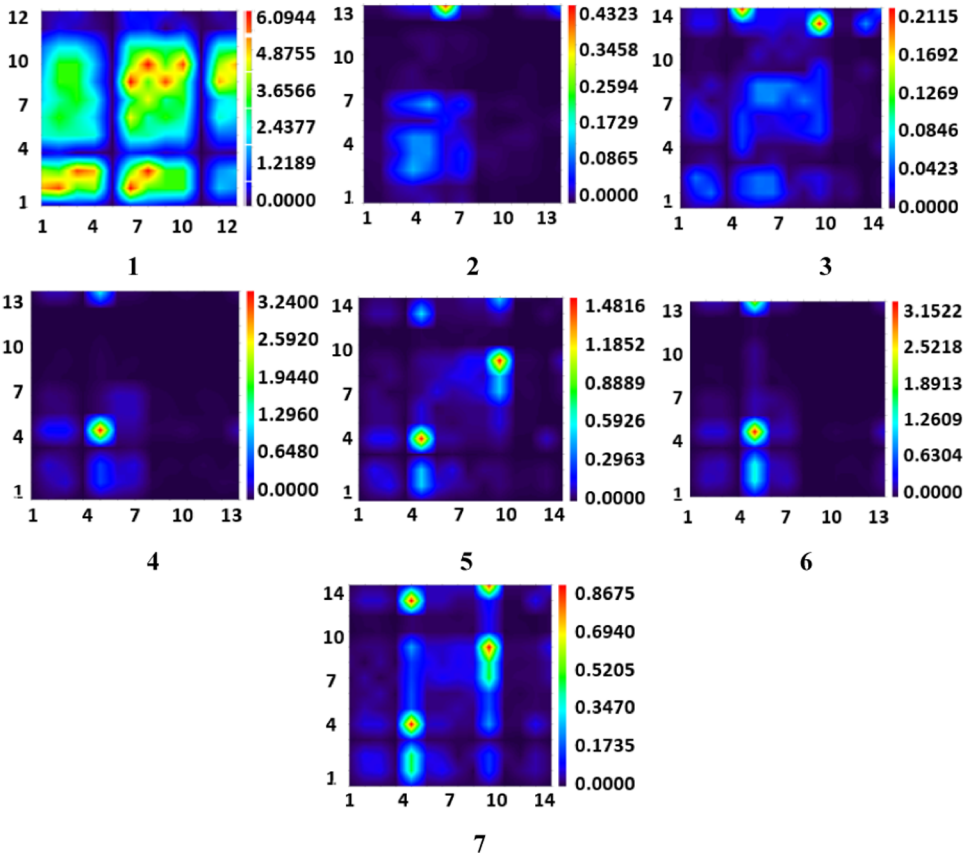

Figure 6. Simulated transition density matrix connected with the lowest excited states of **1**−**7** (the hydrogen atoms of all systems are omitted), and the color bars are given on the right.

5. This observation corroborates with the hole and electron isosurface map, but in molecules **3**, **5**, and **7**, electrons are holes are also present on the isosurface of the diagonal at 5 and 10 positions, respectively, and the electron density is very high in the order of **1** < **2** < **3** < **4** < **5** < **6** < **7**. Furthermore, we can see from the isosurface map that molecule **5** is substantially surrounded by a green isosurface, indicating that this atom does not send electrons to others but does accept electrons from others (Figure 6).

The estimated transition density matrix heat maps further imply that electron transitions in alkali metal-substituted TCD complexes are local excitations (see Figure S2 in the Supporting Information).

4. CONCLUSIONS

We performed quantum chemical calculations on seven TCD derivatives, which were obtained by replacing the H atom of methylene bridge carbon with alkali metals (Li, Na, and K). The calculated results reveal that alkali metal-substituted TCD derivatives affect the absorbance spectrum. Calculated λ_{max} shows an apparent bathochromic change with increasing atomic numbers of alkali metals. Further, the alkali atom contributes to the HOMO of TCD derivatives (**2**−**7**) to form excess electrons, as reflected by the orbital interaction diagram and the DOS curve. The dipole moment and mean polarizability of **2**−**7** are significantly enhanced, which are in accordance with the charge transfer and E_{gap} values, respectively. The β_{tot} value of **7** (β_{tot} = 72059 au) is the largest, which is about 43 times larger than a prototypical second-order NLO molecule of *p*-nitroaniline (β_{tot} = 1675 au). The calculated MP2 results infer that alkali metal-substituted exo-exo-tetracyclo[6.2.1.1^{3,6}.0^{2,7}]dodecane can act as a novel and potential candidate for better organic NLO materials.

■ ASSOCIATED CONTENT

Supporting Information

The Supporting Information is available free of charge at https://pubs.acs.org/doi/10.1021/acsomega.2c07743.

Polarizability and first-order hyperpolarizability of p-NA were calculated at the 6-311+G(d,p) basis set using MP2 and DFT methods with different functionals (PDF)

■ AUTHOR INFORMATION

Corresponding Author

Ajeet Singh − *Department of Chemistry, Prof. Rajendra Singh (Rajju Bhaiya) Institute of Physical Sciences for Study and Research, V.B.S. Purvanchal University, Jaunpur 222003, India*; orcid.org/0000-0001-8073-4909; Email: ajeetmolecule@gmail.com

Authors

Santosh Kumar Yadav − *Department of Chemistry, Prof. Rajendra Singh (Rajju Bhaiya) Institute of Physical Sciences for Study and Research, V.B.S. Purvanchal University, Jaunpur 222003, India*

Snehasis Bhunia − *Department of Chemistry, National Taiwan University, Taipei 10617, Taiwan (R.O.C.)*

Rajneesh Kumar − *Department of Chemistry, Prof. Rajendra Singh (Rajju Bhaiya) Institute of Physical Sciences for Study*

https://doi.org/10.1021/acsomega.2c07743
ACS Omega 2023, 8, 7978−7988

and Research, V.B.S. Purvanchal University, Jaunpur 222003, India

Ritu Seth − *Department of Chemistry, Prof. Rajendra Singh (Rajju Bhaiya) Institute of Physical Sciences for Study and Research, V.B.S. Purvanchal University, Jaunpur 222003, India*

Complete contact information is available at: https://pubs.acs.org/10.1021/acsomega.2c07743

Notes

The authors declare no competing financial interest.

■ ACKNOWLEDGMENTS

A.S. acknowledges SERB, New Delhi (Ref No.: CRG/2019/001032) for financial help under the core research grant. S.K.Y. thanks UGC-India for financial support for the junior research fellowship grant.

■ REFERENCES

(1) Eaton, D. F. Nonlinear Optical Materials. *Science* **1991**, *253*, 281−287.

(2) Zyss, J.; Ledoux, I. Nonlinear Optics in Multipolar Media: Theory and Experiments. *Chem. Rev.* **1994**, *94*, 77−105.

(3) Hu, Z.-Y.; Fort, A.; Barzoukas, M.; Jen, A. K.-Y.; Barlow, S.; Marder, S. R. Trends in Optical Nonlinearity and Thermal Stability in Electrooptic Chromophores Based upon the 3-(Dicyanomethylene)-2, 3-Dihydrobenzothiophene-1, 1-Dioxide Acceptor. *J. Phys. Chem. B* **2004**, *108*, 8626−8630.

(4) Green, M. L. H.; Marder, S. R.; Thompson, M. E.; Bandy, J. A.; Bloor, D.; Kolinsky, P. V.; Jones, R. J. Synthesis and Structure of (Cis)-[1-Ferrocenyl-2-(4-Nitrophenyl) Ethylene], an Organotransition Metal Compound with a Large Second-Order Optical Nonlinearity. *Nature* **1987**, *330*, 360−362.

(5) Di Bella, S. Second-Order Nonlinear Optical Properties of Transition Metal Complexes. *Chem. Soc. Rev.* **2001**, *30*, 355−366.

(6) Yan, H.; Li, X.; Chandra, B.; Tulevski, G.; Wu, Y.; Freitag, M.; Zhu, W.; Avouris, P.; Xia, F. Tunable Infrared Plasmonic Devices Using Graphene/Insulator Stacks. *Nat. Nanotechnol.* **2012**, *7*, 330−334.

(7) Chen, K. J.; Laurent, A. D.; Jacquemin, D. Strategies for Designing Diarylethenes as Efficient Nonlinear Optical Switches. *J. Phys. Chem. C* **2014**, *118*, 4334−4345.

(8) Máthé, L.; Onyenegecha, C. P.; Farcaş, A.-A.; Pioraş-Ţimbolmaş, L.-M.; Solaimani, M.; Hassanabadi, H. Linear and Nonlinear Optical Properties in Spherical Quantum Dots: Inversely Quadratic Hellmann Potential. *Phys. Lett. A* **2021**, *397*, No. 127262.

(9) Meyers, F.; Marder, S. R.; Pierce, B. M.; Bredas, J.-L. Electric Field Modulated Nonlinear Optical Properties of Donor-Acceptor Polyenes: Sum-over-States Investigation of the Relationship between Molecular Polarizabilities (α, β, and γ) and Bond Length Alternation. *J. Am. Chem. Soc.* **1994**, *116*, 10703−10714.

(10) Kukkonen, E.; Lahtinen, E.; Myllyperkiö, P.; Konu, J.; Haukka, M. Three-Dimensional Printing of Nonlinear Optical Lenses. *ACS Omega* **2018**, *3*, 11558−11561.

(11) Van Cleuvenbergen, S.; Asselberghs, I.; Garcia-Frutos, E. M.; Gomez-Lor, B.; Clays, K.; Perez-Moreno, J. Dispersion Overwhelms Charge Transfer in Determining the Magnitude of the First Hyperpolarizability in Triindole Octupoles. *J. Phys. Chem. C* **2012**, *116*, 12312−12321.

(12) Blanchard-Desce, M.; Alain, V.; Bedworth, P. V.; Marder, S. R.; Fort, A.; Runser, C.; Barzoukas, M.; Lebus, S.; Wortmann, R. Large Quadratic Hyperpolarizabilities with Donor−Acceptor Polyenes Exhibiting Optimum Bond Length Alternation: Correlation between Structure and Hyperpolarizability. *Chem.−Eur. J.* **1997**, *3*, 1091−1104.

(13) Coe, B. J.; Jones, L. A.; Harris, J. A.; Brunschwig, B. S.; Asselberghs, I.; Clays, K.; Persoons, A. Highly Unusual Effects of π-Conjugation Extension on the Molecular Linear and Quadratic Nonlinear Optical Properties of Ruthenium (II) Ammine Complexes. *J. Am. Chem. Soc.* **2003**, *125*, 862−863.

(14) Serra-Crespo, P.; van der Veen, M. A.; Van Der Veen, M. A.; Gobechiya, E.; Houthoofd, K.; Filinchuk, Y.; Kirschhock, C. E.; Martens, J. A.; Sels, B. F.; De Vos, D. E.; Kapteijn, F. NH_2-MIL-53 (Al): A High-Contrast Reversible Solid-State Nonlinear Optical Switch. *J. Am. Chem. Soc.* **2012**, *134*, 8314−8317.

(15) Coe, B. J.; Foxon, S. P.; Harper, E. C.; Helliwell, M.; Raftery, J.; Swanson, C. A.; Brunschwig, B. S.; Clays, K.; Franz, E.; Garin, J.; et al. Evolution of Linear Absorption and Nonlinear Optical Properties in V-Shaped Ruthenium (II)-Based Chromophores. *J. Am. Chem. Soc.* **2010**, *132*, 1706−1723.

(16) Bibi, A.; Muhammad, S.; UrRehman, S.; Bibi, S.; Bashir, S.; Ayub, K.; Adnan, M.; Khalid, M. Chemically Modified Quinoidal Oligothiophenes for Enhanced Linear and Third-Order Nonlinear Optical Properties. *ACS Omega* **2021**, *6*, 24602.

(17) Nakano, M.; Fujita, H.; Takahata, M.; Yamaguchi, K. Theoretical Study on Second Hyperpolarizabilities of Phenylacetylene Dendrimer: Toward an Understanding of Structure- Property Relation in NLO Responses of Fractal Antenna Dendrimers. *J. Am. Chem. Soc.* **2002**, *124*, 9648−9655.

(18) Xu, H.-L.; Li, Z.-R.; Wu, D.; Wang, B.-Q.; Li, Y.; Gu, F. L.; Aoki, Y. Structures and Large NLO Responses of New Electrides: Li-Doped Fluorocarbon Chain. *J. Am. Chem. Soc.* **2007**, *129*, 2967−2970.

(19) Champagne, B.; Plaquet, A.; Pozzo, J.-L.; Rodriguez, V.; Castet, F. Nonlinear Optical Molecular Switches as Selective Cation Sensors. *J. Am. Chem. Soc.* **2012**, *134*, 8101−8103.

(20) Wu, H.-Q.; Zhong, R.-L.; Kan, Y.-H.; Sun, S.-L.; Zhang, M.; Xu, H.-L.; Su, Z.-M. After the Electronic Field: Structure, Bonding, and the First Hyperpolarizability of HArF. *J. Comput. Chem.* **2013**, *34*, 952−957.

(21) Karamanis, P.; Pouchan, C. Fullerene−C_{60} in Contact with Alkali Metal Clusters: Prototype Nano-Objects of Enhanced First Hyperpolarizabilities. *J. Phys. Chem. C* **2012**, *116*, 11808−11819.

(22) Koukaras, E. N.; Zdetsis, A. D.; Karamanis, P.; Pouchan, C.; Avramopoulos, A.; Papadopoulos, M. G. Structural and Static Electric Response Properties of Highly Symmetric Lithiated Silicon Cages: Theoretical Predictions. *J. Comput. Chem.* **2012**, *33*, 1068−1079.

(23) Deb, J.; Paul, D.; Sarkar, U. Density Functional Theory Investigation of Nonlinear Optical Properties of T-Graphene Quantum Dots. *J. Phys. Chem. A* **2020**, *124*, 1312−1320.

(24) Chen, W.; Li, Z.-R.; Wu, D.; Li, R.-Y.; Sun, C.-C. Theoretical Investigation of the Large Nonlinear Optical Properties of $(HCN)_n$ Clusters with Li Atom. *J. Phys. Chem. B* **2005**, *109*, 601−608.

(25) Srivastava, A.; Mishra, R.; Kumar, S.; Dev, K.; Tandon, P.; Maurya, R. Molecular Structure, Spectral Investigation (^{1}H NMR, ^{13}C NMR, UV−Visible, FT-IR, FT-Raman), NBO, Intramolecular Hydrogen Bonding, Chemical Reactivity and First Hyperpolarizability Analysis of Formononetin [7-Hydroxy-3 (4-Methoxyphenyl) Chromone]: A Quantum Chemical Study. *J. Mol. Struct.* **2015**, *1084*, 55−73.

(26) De La Torre, G.; Vázquez, P.; Agullo-Lopez, F.; Torres, T. Role of Structural Factors in the Nonlinear Optical Properties of Phthalocyanines and Related Compounds. *Chem. Rev.* **2004**, *104*, 3723−3750.

(27) Kanis, D. R.; Ratner, M. A.; Marks, T. J. Design and Construction of Molecular Assemblies with Large Second-Order Optical Nonlinearities. Quantum Chemical Aspects. *Chem. Rev.* **1994**, *94*, 195−242.

(28) Kumar, R.; Yadav, S. K.; Seth, R.; Singh, A. Designing of Gigantic First-Order Hyperpolarizability Molecules via Joining the Promising Organic Fragments: A DFT Study. *J. Mol. Model.* **2022**, *29*, 1−11.

(29) Zhong, R.-L.; Xu, H.-L.; Li, Z.-R.; Su, Z.-M. Role of Excess Electrons in Nonlinear Optical Response. *J. Phys. Chem. Lett.* **2015**, *6*, 612−619.

(30) Sun, W.-M.; Li, X.-H.; Wu, J.; Lan, J.-M.; Li, C.-Y.; Wu, D.; Li, Y.; Li, Z.-R. Can Coinage Metal Atoms Be Capable of Serving as an

Excess Electron Source of Alkalides with Considerable Nonlinear Optical Responses? *Inorg. Chem.* **2017**, *56*, 4594−4600.
(31) Srivastava, A. K. Lithiated Graphene Quantum Dot and Its Nonlinear Optical Properties Modulated by a Single Alkali Atom: A Theoretical Perspective. *Inorg. Chem.* **2021**, *60*, 3131−3138.
(32) Wang, Y.-F.; Wang, J.-J.; Li, J.; Liu, X.-X.; Wang, Z.-J.; Huang, J.; Li, Z.-R. From an Electride-like Super Alkali Earth Atom to a Superalkalide or Superalkali Electride: M $(HF)_3$ M (M = Na or Li) as Field-Induced Excellent Inorganic NLO Molecular Switches. *J. Mater. Chem. C* **2021**, *9*, 14885−14896.
(33) Naeem, J.; Bano, R.; Ayub, K.; Mahmood, T.; Tabassum, S.; Arooj, A.; Gilani, M. A. Assessment of Alkali and Alkaline Earth Metals Doped Cubanes as High-Performance Nonlinear Optical Materials by First-Principles Study. *J. Sci. Adv. Mater. Devices* **2022**, *7*, No. 100457.
(34) Hou, J.; Jiang, D.; Qin, J.; Duan, Q.; et al. Alkaline-Earthide: A New Class of Excess Electron Compounds Li-$C_6H_6F_6$-M (M = Be, Mg and Ca) with Extremely Large Nonlinear Optical Responses. *Chem. Phys. Lett.* **2018**, *711*, 55−59.
(35) Wagner, M. J.; Dye, J. L. In *Molecular Recognition: Receptors for Cationic Guests*, Gokel, G. W.1996.
(36) Ahsin, A.; Ayub, K. Superalkali-Based Alkalides Li_3O@[12-Crown-4] M (Where M = Li, Na, and K) with Remarkable Static and Dynamic NLO Properties; A DFT Study. *Mater. Sci. Semicond. Process.* **2022**, *138*, No. 106254.
(37) Li, X.-H.; Zhang, X.-L.; Chen, Q.-H.; Zhang, L.; Chen, J.-H.; Wu, D.; Sun, W.-M.; Li, Z.-R. Coinage Metalides: A New Class of Excess Electron Compounds with High Stability and Large Nonlinear Optical Responses. *Phys. Chem. Chem. Phys.* **2020**, *22*, 8476−8484.
(38) Khan, M. U.; Hussain, S.; Asghar, M. A.; Munawar, K. S.; Khera, R. A.; Imran, M.; Ibrahim, M. M.; Hessien, M. M.; Mersal, G. A. Exploration of Nonlinear Optical Properties for the First Theoretical Framework of Non-Fullerene DTS $(FBTTh_2)_2$-Based Derivatives. *ACS Omega* **2022**, *7*, 18027−18040.
(39) Chen, W.; Li, Z.-R.; Wu, D.; Gu, F.-L.; Hao, X.-Y.; Wang, B.-Q.; Li, R.-J.; Sun, C.-C. The Static Polarizability and First Hyperpolarizability of the Water Trimer Anion: Ab Initio Study. *J. Chem. Phys.* **2004**, *121*, 10489−10494.
(40) Li, Y.; Li, Z.-R.; Wu, D.; Li, R.-Y.; Hao, X.-Y.; Sun, C.-C. An Ab Initio Prediction of the Extraordinary Static First Hyperpolarizability for the Electron-Solvated Cluster $(FH)_2$ {e}(HF). *J. Phys. Chem. B* **2004**, *108*, 3145−3148.
(41) Khalid, M.; Zafar, M.; Hussain, S.; Asghar, M. A.; Khera, R. A.; Imran, M.; Abookleesh, F. L.; Akram, M. Y.; Ullah, A. Influence of End-Capped Modifications in the Nonlinear Optical Amplitude of Nonfullerene-Based Chromophores with a D- π−A Architecture: A DFT/TDDFT Study. *ACS Omega* **2022**, *7*, 23532−23548.
(42) Wu, H.-Q.; Zhong, R.-L.; Sun, S.-L.; Xu, H.-L.; Su, Z.-M. Alkali Metals-Substituted Adamantanes Lead to Visible Light Absorption: Large First Hyperpolarizability. *J. Phys. Chem. C* **2014**, *118*, 6952−6958.
(43) Holl, M. G.; Pitts, C. R.; Lectka, T. Fluorine in a C- F Bond as the Key to Cage Formation. *Angew. Chem., Int. Ed.* **2018**, *57*, 2758−2766.
(44) Sangeetha, P.; Diravidamani, B.; Dhandapani, A.; Suresh, M.; Uthayakumar, M.; Shinde, V. Structural, Spectral, DFT and Z-Scan Analysis of (E)-4-Fluoro-N′(3, 4, 5-Trimethoxybenzylidene) Benzohydrazide for Optoelectronics Applications. *Optik* **2022**, *266*, No. 169602.
(45) Kivelson, D.; Winstein, S.; Bruck, P.; Hansen, R. L.; Sterically Increased, C. H. Stretching Frequencies in Fused Bicycloheptane and Half-Cage Structures[1,2]. *J. Am. Chem. Soc.* **1961**, *83*, 2938−2944.
(46) Ermer, O. Structure of Two Highly Strained Tetracyclododecanes. *Angew. Chem. Int. Ed. Engl.* **1977**, *16*, 798−799.
(47) Lowe, A. J.; Long, B. M.; Pfeffer, F. M. Conformationally Preorganised Hosts for Anions Using Norbornane and Fused [n] Polynorbornane Frameworks. *Chem. Commun.* **2013**, *49*, 3376−3388.
(48) Singh, A.; Ganguly, B. Rational Design and First-Principles Studies toward the Remote Substituent Effects on a Novel Tetracyclic Proton Sponge. *J. Phys. Chem. A* **2007**, *111*, 6468−6471.
(49) Frisch, M. A.; Trucks, G. W.; Schlegel, H. B.; Scuseria, G. E.; Robb, M. A.; Cheeseman, J. R.; Scalmani, G.; Barone, V.; Petersson, G. A.; Nakatsuji, H.. *Gaussian 16*, 2016.
(50) Reed, A. E.; Weinstock, R. B.; Weinhold, F. Natural Population Analysis. *J. Chem. Phys.* **1985**, *83*, 735−746.
(51) Skwara, B.; Góra, R. W.; Zalesny, R.; Lipkowski, P.; Bartkowiak, W.; Reis, H.; Papadopoulos, M. G.; Luis, J. M.; Kirtman, B. Electronic Structure, Bonding, Spectra, and Linear and Nonlinear Electric Properties of Ti@C_{28}. *J. Phys. Chem. A* **2011**, *115*, 10370−10381.
(52) Chen, L.; Yu, G.; Chen, W.; Tu, C.; Zhao, X.; Huang, X. Constructing a Mixed π-Conjugated Bridge to Effectively Enhance the Nonlinear Optical Response in the Möbius Cyclacene-Based Systems. *Phys. Chem. Chem. Phys.* **2014**, *16*, 10933−10942.
(53) Belz, J.; Haust, J.; Müller, M. J.; Eberheim, K.; Schwan, S.; Gowrisankar, S.; Hüppe, F.; Beyer, A.; Schreiner, P. R.; Mollenhauer, D.; et al. Adamantanes as White-Light Emitters: Controlling the Arrangement and Functionality by External Coulomb Forces. *J. Phys. Chem. C* **2022**, *126*, 9843−9854.
(54) O'boyle, N. M.; Tenderholt, A. L.; Langner, K. M. Cclib: A Library for Package-Independent Computational Chemistry Algorithms. *J. Comput. Chem.* **2008**, *29*, 839−845.
(55) Yanai, T.; Tew, D. P.; Handy, N. C. A New Hybrid Exchange−Correlation Functional Using the Coulomb-Attenuating Method (CAM-B3LYP). *Chem. Phys. Lett.* **2004**, *393*, 51−57.
(56) Castro-Alvarez, A.; Carneros, H.; Sánchez, D.; Vilarrasa, J. Importance of the Electron Correlation and Dispersion Corrections in Calculations Involving Enamines, Hemiaminals, and Aminals. Comparison of B3LYP, M06-2X, MP2, and CCSD Results with Experimental Data. *J. Org. Chem.* **2015**, *80*, 11977−11985.
(57) Chai, J.-D.; Head-Gordon, M. Long-Range Corrected Hybrid Density Functionals with Damped Atom−Atom Dispersion Corrections. *Phys. Chem. Chem. Phys.* **2008**, *10*, 6615−6620.
(58) Austin, A.; Petersson, G. A.; Frisch, M. J.; Dobek, F. J.; Scalmani, G.; Throssell, K. A Density Functional with Spherical Atom Dispersion Terms. *J. Chem. Theory Comput.* **2012**, *8*, 4989−5007.
(59) Grimme, S.; Ehrlich, S.; Goerigk, L. Effect of the Damping Function in Dispersion Corrected Density Functional Theory. *J. Comput. Chem.* **2011**, *32*, 1456−1465.
(60) Grimme, S. Semiempirical GGA-Type Density Functional Constructed with a Long-Range Dispersion Correction. *J. Comput. Chem.* **2006**, *27*, 1787−1799.
(61) Jadhav, A. G.; Rhyman, L.; Alswaidan, I. A.; Ramasami, P.; Sekar, N. Spectroscopic and DFT Approach for Structure Property Relationship of Red Emitting Rhodamine Analogues: A Study of Linear and Nonlinear Optical Properties. *Comput. Theor. Chem.* **2018**, *1131*, 1−12.
(62) Ayare, N. N.; Shukla, V. K.; Sekar, N. Charge Transfer and Nonlinear Optical Properties of Anthraquinone D-π-A Dyes in Relation with the DFT Based Molecular Descriptors and Perturbational Potential. *Comput. Theor. Chem.* **2020**, *1174*, No. 112712.
(63) Zouaoui-Rabah, M.; Sekkal-Rahal, M.; Djilani-Kobibi, F.; Elhorri, A. M.; Springborg, M. Performance of Hybrid DFT Compared to MP2 Methods in Calculating Nonlinear Optical Properties of Divinylpyrene Derivative Molecules. *J. Phys. Chem. A* **2016**, *120*, 8843−8852.
(64) Elhorri, A.; Zouaoui-Rabah, M. NLO Response of Derivatives of Benzene, Stilbene and Diphenylacetylene: MP2 and DFT Calculations. *Chin. J. Chem. Eng.* **2017**, *25*, 800−808.
(65) Chołuj, M.; Kozłowska, J.; Bartkowiak, W. Benchmarking DFT Methods on Linear and Nonlinear Electric Properties of Spatially Confined Molecules. *Int. J. Quantum Chem.* **2018**, *118*, No. e25666.
(66) Champagne, B.; Botek, E.; Nakano, M.; Nitta, T.; Yamaguchi, K. Basis Set and Electron Correlation Effects on the Polarizability and Second Hyperpolarizability of Model Open-Shell π-Conjugated Systems. *J. Chem. Phys.* **2005**, *122*, No. 114315.

https://doi.org/10.1021/acsomega.2c07743
ACS Omega 2023, 8, 7978−7988

(67) Nakano, M.; Kishi, R.; Nitta, T.; Kubo, T.; Nakasuji, K.; Kamada, K.; Ohta, K.; Champagne, B.; Botek, E.; Yamaguchi, K. Second Hyperpolarizability (γ) of Singlet Diradical System: Dependence of γ on the Diradical Character. *J. Phys. Chem. A* **2005**, *109*, 885−891.
(68) Haroon, M.; Janjua, M. R. S. A. Computationally Assisted Design and Prediction of Remarkably Boosted NLO Response of Organoimido-Substituted Hexamolybdates. *J. Phys. Org. Chem.* **2022**, *35*, No. e4353.
(69) Xu, H.-L.; Li, Z.-R.; Su, Z.-M.; Muhammad, S.; Gu, F. L.; Harigaya, K. Knot-Isomers of Mobius Cyclacene: How Does the Number of Knots Influence the Structure and First Hyperpolarizability? *J. Phys. Chem. C* **2009**, *113*, 15380−15383.
(70) Zhang, J.; Zhang, F.-Y.; Su, Z.-M.; Xu, H.-L. Pyramid-Like Au_2-CNC under an External Electric Field: Charge Transfer, UV−Vis Absorption Spectra, and Nonlinear Optical Property. *J. Phys. Chem. C* **2022**, *126*, 16236−16242.
(71) Lu, T.; Chen, F. Multiwfn: A Multifunctional Wavefunction Analyzer. *J. Comput. Chem.* **2012**, *33*, 580−592.
(72) Li, Y.; Ullrich, C. A. Time-Dependent Transition Density Matrix. *Chem. Phys.* **2011**, *391*, 157−163.

https://doi.org/10.1021/acsomega.2c07743
ACS Omega 2023, 8, 7978−7988